Sulfate and Carboxylate Suppress the Formation of ClNO$_2$ at Atmospheric Interfaces

Sean Staudt,[†] Joseph R. Gord,[†] Natalia V. Karimova,[‡] Erin E. McDuffie,[§,∥,⊥,◆] Steven S. Brown,[§,⊥] R. Benny Gerber,[‡,#] Gilbert M. Nathanson,*[,†] and Timothy H. Bertram*[,†,∇,○]

[†]Department of Chemistry, University of Wisconsin—Madison, Madison, Wisconsin 53706, United States
[‡]Department of Chemistry, University of California, Irvine, California 92697, United States
[§]Chemical Sciences Division, National Oceanic and Atmospheric Administration, Boulder, Colorado 80305, United States
[∥]Cooperative Institute for Research in Environmental Sciences, University of Colorado, Boulder, Colorado 80309, United States
[⊥]Department of Chemistry, University of Colorado, Boulder, Colorado 80309, United States
[#]Institute of Chemistry and Fritz Haber Research Center, Hebrew University of Jerusalem, Jerusalem 91904, Israel
[∇]Department of Atmospheric and Oceanic Sciences, University of Wisconsin—Madison, Madison, Wisconsin 53706, United States
[○]Environmental Chemistry and Technology Program, University of Wisconsin—Madison, Madison, Wisconsin 53706, United States

S *Supporting Information*

ABSTRACT: We report measurements of the nitryl chloride (ClNO$_2$) branching fraction following reactive uptake of N$_2$O$_5$ to mixed organic and inorganic solutions representative of atmospheric interfaces. For sodium chloride containing solutions, mixed with either sodium sulfate (Na$_2$SO$_4$) or sodium acetate (NaAc), the ClNO$_2$ branching fraction (Φ_{ClNO_2}) is suppressed relative to a sodium chloride only solution. In the case of the sulfate-chloride solution, Φ_{ClNO_2} is reduced from 0.85 ± 0.03 (0.5 M NaCl) to 0.32 ± 0.14 upon the addition of 2.0 M Na$_2$SO$_4$. In the case of the acetate-chloride solution, Φ_{ClNO_2} is reduced to 0.18 ± 0.03 upon the addition of 0.5 M NaAc. In contrast, no statistically significant suppression in Φ_{ClNO_2} was observed for the addition of sodium perchlorate up to 3.0 M, implying that an increase in ionic strength of the solution does not necessitate a reduction in Φ_{ClNO_2}. We

suggest that the reduction in Φ_{ClNO_2} may result from a direct reaction between SO$_4^{2-}$ (and Ac$^-$) with NO$_2^+$ (or NO$_2^+$NO$_3^-$) which competes with the NO$_2^+$ + Cl$^-$ reaction that produces ClNO$_2$. The dependence of Φ_{ClNO_2} on SO$_4^{2-}$ and Ac$^-$ is compared with both a time-dependent reaction-diffusion model and recent field observations, suggesting that the reaction rate of SO$_4^{2-}$ (or Ac$^-$) with NO$_2^+$ would need to be similar in magnitude to the rate of the NO$_2^+$ + Cl$^-$ reaction to explain the observed suppression in Φ_{ClNO_2}. We show that the dependence of Φ_{ClNO_2} on particulate sulfate and carboxylate can be readily incorporated into existing parametrizations of ClNO$_2$ heterogeneous chemistry. The results presented here indicate that anions which are ubiquitous in atmospheric aerosol, yet commonly considered to be unreactive, may regulate the production of reactive gases such as ClNO$_2$.

KEYWORDS: *Heterogeneous and multiphase chemistry, N$_2$O$_5$, ClNO$_2$ yield, aerosol particles, air pollution, chlorine activation, reactive nitrogen, nocturnal nitrogen oxides*
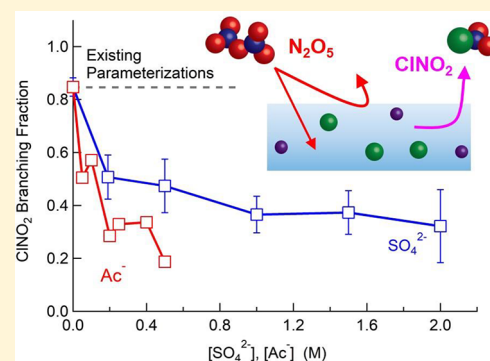
1. INTRODUCTION

Aerosol particles catalyze both the production and loss of reactive gases in Earth's atmosphere with consequent impacts on air quality and the lifetime of greenhouse gases.[1] Heterogeneous and multiphase reactions of dinitrogen pentoxide (N$_2$O$_5$) have garnered the attention of the atmospheric chemistry community for decades as hydrolysis at atmospheric interfaces is an efficient, yet highly variable, termination mechanism for nitrogen oxides.[2] The reactive

uptake of N$_2$O$_5$ to chloride containing particles results in the production and subsequent evaporation of nitryl chloride (ClNO$_2$), a photolabile reservoir for both nitrogen dioxide and chlorine radicals.[3−6]
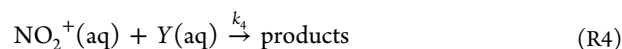
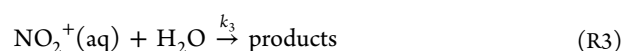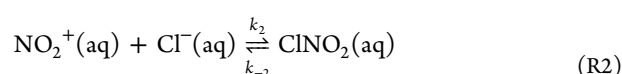The fraction of N_2O_5 that is converted to $ClNO_2$, following reactive uptake to aqueous interfaces, depends strongly on the chloride concentration.[3] The molecular level details of the reaction mechanism that links N_2O_5 reactive uptake with $ClNO_2$ production in atmospheric particles are unknown, but the following mechanism (reactions R1−R4), involving the formation of a transient nitronium ion (NO_2^+), where $NO_2^+(aq)$ represents either the individually solvated NO_2^+ ion or the contact ion pair $(NO_2^+NO_3^-)$.[7] This mechanism is consistent with laboratory and field observations of the N_2O_5 reactive uptake coefficient, $\gamma(N_2O_5)$, and the $ClNO_2$ branching fraction, Φ_{ClNO_2}.[2] For simplicity, we interpret the measurements described here in the context of the two-step reaction mechanism (reactions R1 and R2) shown below.

$$N_2O_5(aq) \underset{k_{-1}}{\overset{k_1}{\rightleftharpoons}} NO_2^+(aq) + NO_3^-(aq) \tag{R1}$$

$$NO_2^+(aq) + Cl^-(aq) \underset{k_{-2}}{\overset{k_2}{\rightleftharpoons}} ClNO_2(aq) \tag{R2}$$

$$NO_2^+(aq) + H_2O \overset{k_3}{\rightarrow} products \tag{R3}$$

$$NO_2^+(aq) + Y(aq) \overset{k_4}{\rightarrow} products \tag{R4}$$
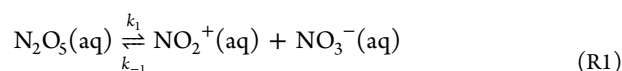
There are no direct measurements of either the hydrolysis rate of N_2O_5 (reaction R1) or the subsequent aqueous phase reactions involving NO_2^+ (reactions R2−R4). However, recent theoretical calculations of the competing substitution and hydrolysis reactions in three-body clusters $(N_2O_5/H_2O/Cl^-)$ provide a microscopic picture of the mechanisms and time scales for these reactions.[8] Concurrent, laboratory measurements of the gas-phase loss of N_2O_5 and the evaporation of $ClNO_2$ from chloride containing solutions have been used to infer the ratio of the NO_2^+ reaction rates (k_2/k_3), yielding ratios ranging from 450 ± 100 to 836 ± 32.[3,9−11]

Heal et al. first suggested that reactions of NO_2^+ with soluble organic compounds were competitive with $NO_2^+ + H_2O$ (reaction R3).[12] In the case of phenol, the ratio of the rate constants, $k(NO_2^+ + phenol)/k(NO_2^+ + H_2O)$, was determined to be in excess of 1000 (at pH = 10), suggesting that other chemical constituents in aerosol particles could alter Φ_{ClNO_2} (reaction R4). More recently, Ryder et al. showed that Φ_{ClNO_2} measured for organic-containing ocean water samples was significantly lower $(0.16 \pm 0.05 < \Phi_{ClNO_2} < 0.30 \pm 0.08)$ than that measured for 0.5 M chloride solutions (0.82 ± 0.05).[10]

Recent field investigations have focused on reconciling atmospheric determinations of Φ_{ClNO_2} with model predictions.[5,6,13−15] In these analyses, predictions of Φ_{ClNO_2} are derived from the laboratory-determined dependence of Φ_{ClNO_2} on the molar ratio of aerosol chloride to water, using coincident measurements of aerosol chloride mass and calculation of aerosol liquid water content as the input parameters. In both coastal and continental airmasses, calculations of Φ_{ClNO_2} generally overpredict atmospheric determinations of Φ_{ClNO_2}.[13,14] The discrepancy could be a result of (1) model approximations regarding particle-to-particle variability in the chloride concentration of aerosol particles, (2) challenges in the measurement and calculation of total aerosol chloride and water concentrations, (3) reactions

of NO_2^+ with nucleophiles other than Cl^- that compete with $ClNO_2$ formation, (4) dry deposition of $ClNO_2$,[16] and/or (5) subsequent reactions of $ClNO_2$ within the aerosol particle prior to evaporation.

In this study, we build on the initial work of Ryder et al. and explore potential reactions of N_2O_5 with other strong nucleophiles that are present in ambient aerosol.[17] We describe laboratory measurements of Φ_{ClNO_2} for mixed organic and inorganic solutions containing sulfate and carboxylates, which are ubiquitous in ambient aerosol particles.[17] These solutions contain the sodium salts of chloride mixed with sulfate or acetate (a proxy for carboxylates) at concentrations ranging between 0 and 3 M, representative of deliquesced ambient aerosol.[13] Determinations of Φ_{ClNO_2} using mixtures of sodium chloride and sodium perchlorate were conducted as control experiments. We interpret the observations with a coupled reaction-diffusion model to determine relative reaction rates for NO_2^+ with sulfate and acetate ions, referenced to the reaction of NO_2^+ with Cl^-. The results of these laboratory studies are compared with prior estimates of Φ_{ClNO_2} derived from field experiments.[13]

2. EXPERIMENTAL SECTION

The $ClNO_2$ branching fraction (Φ_{ClNO_2}), following the reactive uptake of N_2O_5, was measured for a series of mixed organic and inorganic solutions utilizing the approach of Roberts et al.[11] In this section, we briefly describe solution preparation and the experimental procedure for determination of Φ_{ClNO_2}.

2.1. Materials. Sodium sulfate (Sigma-Aldrich, ACS Reagent, ≥99.0%, anhydrous, granular), sodium perchlorate (Sigma-Aldrich, ACS Reagent, ≥98.0%), and sodium acetate (Sigma-Aldrich, ACS Reagent, ≥99.0%) solutions were prepared in 0.5 M sodium chloride (Sigma-Aldrich, ACS Reagent, ≥99.0%) in deuterated water (Aldrich Chemistry, 99.9%). Solute concentrations used in this study ranged between 0.0 and 3.0 M due to solubility constraints in 0.5 M $NaCl/D_2O$ (Table 1). For each solution, the pH was high enough (pH > 5.3 and pH > 7.3 for the $NaCl/Na_2SO_4$ and NaCl/NaAc experiments, respectively) that the sulfate, acetate, and perchlorate anions dominated over their protonated states by at least 99:1. Trace amounts of acetic acid were observed in the gas phase during the NaCl/NaAc experiments, suggesting either an impurity in the NaAc salt or slight acidification of the samples by CO_2 prior to the measurement.

N_2O_5 was generated in situ following the procedure described in Bertram et al.[18] Briefly, ultrapure zero air and ultrahigh purity nitrogen, each dried by passing the gas stream through a potassium hydroxide trap, were mixed prior to illumination by a low-pressure mercury pen lamp (Jelight 95−2100−1), generating a stable concentration of ozone (O_3). The $N_2/O_2/O_3$ flow was then mixed with nitrogen dioxide delivered from a $53.92 \pm 2\%$ ppm of NO_2 in N_2 compressed gas cylinder (Airgas) directly prior to mixing in a dark, glass reaction cell for approximately 100 s. The resulting O_3, NO_2, NO_3, and N_2O_5 concentrations in the 100 sccm flow are estimated to be 180, 1300, 0.017, and 12 ppb, respectively, based on measurements of changes in the O_3 concentration as in Bertram et al.[18]

2.2. Surface Tension Measurements. The surface tensions of solutions containing Na_2SO_4, $NaClO_4$, and NaAc in 0.5 M NaCl were measured using the Wilhelmy plate

Table 1. Solution Concentrations and Measured $ClNO_2$ Branching Fractions (Φ_{ClNO_2}) for Systems Investigated in This Study[a]

solute dissolved in 0.5 M NaCl/D_2O	concentration (M)	Φ_{ClNO_2} (Figure 2)	replicates Φ_{ClNO_2} (N)
blank (0.5 M NaCl in D_2O only)	$[Cl^-] = 0.5$ M	0.847 ± 0.034	110
sulfate	$[SO_4^{2-}] = 0.19$ M	0.507 ± 0.082	15
sulfate	$[SO_4^{2-}] = 0.5$ M	0.474 ± 0.099	21
sulfate	$[SO_4^{2-}] = 1.0$ M	0.366 ± 0.068	26
sulfate	$[SO_4^{2-}] = 1.5$ M	0.373 ± 0.081	24
sulfate	$[SO_4^{2-}] = 2.0$ M	0.322 ± 0.135	3
acetate	$[Ac^-] = 0.05$ M	0.495 ± 0.098	12
acetate	$[Ac^-] = 0.1$ M	0.560 ± 0.122	18
acetate	$[Ac^-] = 0.2$ M	0.279 ± 0.160	6
acetate	$[Ac^-] = 0.25$ M	0.330 ± 0.051	3
acetate	$[Ac^-] = 0.4$ M	0.323 ± 0.156	11
acetate	$[Ac^-] = 0.5$ M	0.184 ± 0.021	3
perchlorate	$[ClO_4^-] = 0.6875$ M	0.790 ± 0.130	8
perchlorate	$[ClO_4^-] = 1.0$ M	0.676 ± 0.083	6
perchlorate	$[ClO_4^-] = 1.25$ M	0.723 ± 0.105	8
perchlorate	$[ClO_4^-] = 1.5$ M	0.794 ± 0.208	7
perchlorate	$[ClO_4^-] = 2.25$ M	0.849 ± 0.210	6
perchlorate	$[ClO_4^-] = 3.0$ M	1.01 ± 0.13	7

[a]Φ_{ClNO_2} values are the mean of replicate measurements $\pm90\%$ confidence interval.

method. Surface tensions were also measured for each of the pure salt solutions to confirm solution purity and determine the potential for surfactant contaminants to impact measurements of Φ_{ClNO_2}.

As described in the Supporting Information, surface tension measurements revealed that the sodium chloride salt required purification by repeated suctioning of the surface of the solution. After purification, the suctioned 0.5 M NaCl/D_2O solution was then used to prepare the mixed salt solutions. The other salts did not require purification, as verified by surface tension measurements that reproduced literature values.

2.3. Determination of $ClNO_2$ Branching Fraction (Φ_{ClNO_2}). The reaction chambers closely resemble those in Roberts et al.[11] In this study, N_2O_5 is directed through a custom glass reaction chamber containing either an empty polyfluoroalkoxy alkane (PFA) sample holder (the bypass path) or a PFA sample holder containing 6 mL of the test solution (the sample path). The PFA sample holders used in both the bypass and sample pathways were cut from 1.27 cm O.D. PFA tubing into 15.5 cm lengths and milled on one side to create a 13.5 cm opening after insertion of custom-made polytetrafluoroethylene (PTFE) plugs. This design resulted in a reactive surface area of the solution of approximately 10 cm². The absolute humidity of the air in both the sample and bypass paths was matched by the addition of D_2O to the gas stream in the bypass path to account for evaporative loss of D_2O from the sample solution.

Two different chemical ionization mass spectrometers (CIMS) were used in this study, each operating with the same ion chemistry. When available, a time-of-flight mass spectrometer (CI-ToFMS, Aerodyne Research Inc. and Tofwerk AG) was used due to its higher precision and resolving power.[19] Experiments were also conducted using a

quadrupole mass spectrometer (QMS), as in Ryder et al.[10] Both instruments were operated in negative ion mode, utilizing iodide ion chemistry for the selective detection of N_2O_5 and $ClNO_2$ as iodine adducts, $I^-\cdot N_2O_5$ (234.9 m/Q) and $I^-\cdot ClNO_2$ (207.9 m/Q), respectively.[20] In the ion optics region of the CI-QMS, we chose a very weak electric field to maximize sensitivity to iodide analyte adducts. This also resulted in the efficient transmission of larger $I^-\cdot H_2O$ clusters ($I^-\cdot(H_2O)_x$, $x = 0-6$). An undesired consequence of the weak electric field was efficient transmission of the $I^-\cdot HNO_3\cdot H_2O$ cluster ion (207.91 m/Q), which was not separable from $I^-\cdot ClNO_2$ (207.87 m/Q) in the quadrupole mass analyzer. To overcome this, we used D_2O in place of H_2O in all branching fraction experiments, which moved the $I^-\cdot HNO_3\cdot H_2O$ peak to $I^-\cdot DNO_3\cdot D_2O$ (210.91 m/Q).

Data from a typical experiment, where the CIMS alternated sampling between the bypass and sample paths, is shown in Figure 1. The $ClNO_2$ branching fraction (Φ_{ClNO_2}) is defined as
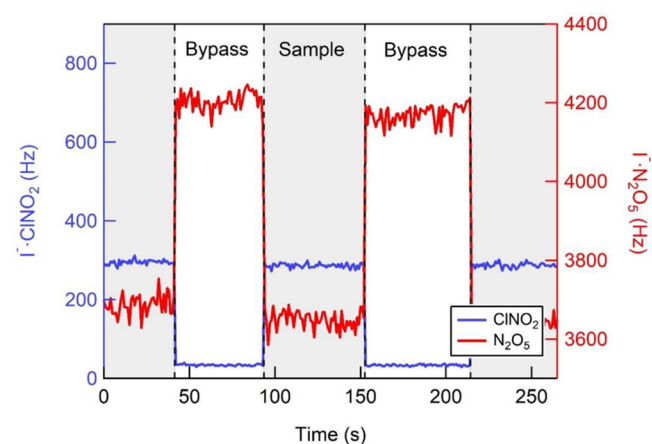

Figure 1. Signal intensities of $ClNO_2$ (measured as $I^-\cdot ClNO_2$ at 207.9 m/Q) and N_2O_5 (measured as $I^-\cdot N_2O_5$ at 234.9 m/Q) when sampling from the flow reactor in the bypass state (no reactive solution) and the sample state (gray shaded regions, reactive Cl^- containing solution), as detected by CI-ToFMS. Assuming every N_2O_5 molecule lost is due to reaction and generation of $ClNO_2$, a sensitivity ratio may be computed for the instruments used in this experiment, as expressed in eq E1.

the ratio of the gas-phase $ClNO_2$ produced relative to N_2O_5 lost to the reactive aqueous solution. This is shown in eq E1, where Φ_{ClNO_2} is the ratio of the change in $ClNO_2$ signal intensity ($\Delta ClNO_2 = ClNO_2$ (sample) $- ClNO_2$ (bypass)) to the change in N_2O_5 signal intensity ($\Delta N_2O_5 = N_2O_5$ (bypass) $- N_2O_5$ (sample)) multiplied by the CIMS sensitivity ratio for each molecule (S_{ClNO_2} and $S_{N_2O_5}$).

$$\Phi_{ClNO_2} = \frac{\Delta ClNO_2}{\Delta N_2O_5} \frac{S_{N_2O_5}}{S_{ClNO_2}} \qquad (E1)$$

N_2O_5 sensitivity for each instrument was determined directly using the N_2O_5 generation technique described in Bertram et al.[18] CIMS sensitivity to $ClNO_2$ was determined by passing N_2O_5 over a concentrated NaCl slurry as in Osthoff et al.[5] Using this approach, Φ_{ClNO_2} was measured as a function of $[Cl^-]$ and fit to a curve as described in Roberts et al.[11] It is important to note that eq E1 does not depend on $\gamma(N_2O_5)$ and that $\gamma(N_2O_5)$ cannot be determined in this experiment due to

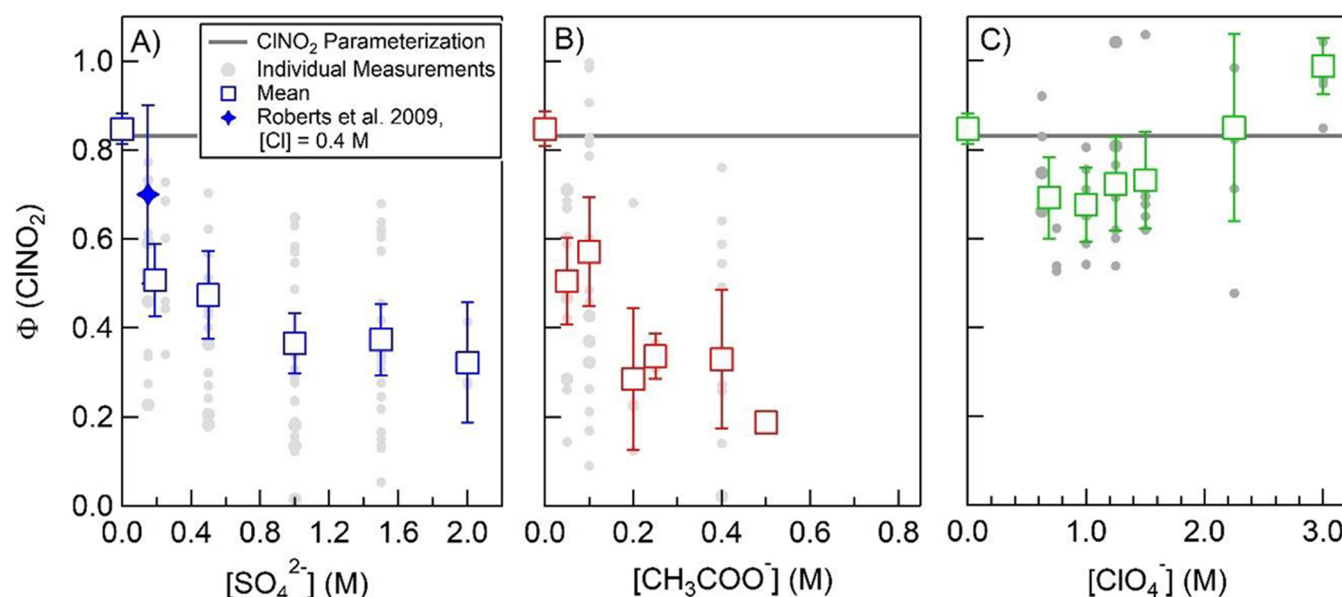**Figure 2.** ClNO$_2$ branching fraction (Φ_{ClNO_2}) for 0.5 M NaCl/D$_2$O solutions with varying concentrations of sodium sulfate (A), sodium acetate (B), and sodium perchlorate (C). The gray dots in each figure represent individual experiments, the squares are the mean of the measurements for each concentration, and the error bar is the 90% confidence interval. The Φ_{ClNO_2} measurement of Roberts et al.[11] conducted on 0.15 M (NH$_4$)$_2$SO$_4$ is included for comparison ([Cl$^-$] = 0.4 M).

gas-phase diffusion limitations. The resulting Φ_{ClNO_2} curves generated for each of the instruments yielded ratios (k_2/k_3 = 531 ± 74) in agreement with prior measurements to within experimental uncertainty.[3,9,11]

3. RESULTS AND DISCUSSION

3.1. ClNO$_2$ Production in Mixed Organic and Inorganic Solutions. In Ryder et al.,[10] we showed that surface-active phenol molecules could suppress the ClNO$_2$ branching fraction (Φ_{ClNO_2}) following the reactive uptake of N$_2$O$_5$ to 0.5 M NaCl solutions containing phenol. Specifically, Φ_{ClNO_2} was reduced from a reported 0.82 ± 0.05 (0.5 M NaCl) to 0.53 ± 0.03 with the addition of 2 mM phenol. We interpreted the suppression in Φ_{ClNO_2} to reflect a competition between Cl$^-$ and phenol for the nitronium ion (NO$_2^+$) formed in the near-surface (<1 nm) hydrolysis of N$_2$O$_5$, the latter reaction resulting in the formation of nitrophenol. This result prompted us to explore potential reactions of N$_2$O$_5$ (hereafter meaning N$_2$O$_5$ and/or NO$_2^+$) with other strong nucleophiles that are omnipresent in ambient aerosol (e.g., sulfate and organic material).[17]

Sodium sulfate (Na$_2$SO$_4$) ranging from 0.0 to 2.0 M (Table 1) was added to 0.5 M NaCl/D$_2$O solutions and Φ_{ClNO_2} was determined via eq E1. As shown in Figure 2A, addition of sodium sulfate led to a suppression in the ClNO$_2$ branching fraction, where Φ_{ClNO_2} was reduced from 0.85 ± 0.03 ([SO$_4^{2-}$] = 0.0 M) to 0.32 ± 0.14 ([SO$_4^{2-}$]$_{bulk}$ = 2.0 M). The squares in Figure 2A represent the mean of multiple measurements (Table 1), and the error bars represent the 90% confidence intervals, derived from the standard error of the mean. The light gray dots indicate individual determinations of Φ_{ClNO_2}. We are aware of only one other determination of Φ_{ClNO_2} in the presence of sulfate. Roberts et al.[11] report Φ_{ClNO_2} = 0.7 ± 0.2 for 0.4 M NaCl in the presence of 0.15 M ammonium sulfate

(Figure 3 of Roberts et al.[11]). Though a different cation, this result is consistent with what is presented here, falling on the steep curve between 0 and 0.19 M sulfate (in 0.5 M NaCl).

Sodium acetate (NaAc) was added to 0.5 M NaCl/D$_2$O solutions to prepare samples with bulk Ac$^-$ concentrations ranging from 0.0 to 0.5 M (Table 1). As shown in Figure 2B, addition of sodium acetate also led to a suppression in the ClNO$_2$ branching fraction, where Φ_{ClNO_2} was reduced from 0.85 ± 0.03 ([Ac$^-$] = 0.0 M) to 0.18 ± 0.03 ([Ac$^-$]$_{bulk}$ = 0.5 M). Φ_{ClNO_2} observed for the equimolar Ac$^-$/Cl$^-$ solutions was more than a factor of 2 smaller than that observed for the equimolar SO$_4^{2-}$/Cl$^-$ solutions (0.47 vs 0.18). Production of Cl$_2$ was not observed in any experiment. Potential causes for the sharp changes in Φ_{ClNO_2} with Na$_2$SO$_4$ and NaAc are discussed in the next section.

3.2. Potential Mechanisms for Suppression in ClNO$_2$ Branching Fraction. We briefly discuss three mechanisms that could be responsible for the observed reduction in Φ_{ClNO_2} in the presence of sodium salts of sulfate and acetate: (1) a reduction in Cl$^-$ reactivity due to a kinetic salt effect or an increase in solution viscosity upon adding salt to the 0.5 M NaCl solution, (2) a reduction in the near-surface Cl$^-$ concentration following the addition of sulfate and acetate anions to solution, and (3) a direct reaction between SO$_4^{2-}$ (or Ac$^-$) and N$_2$O$_5$ that competes with the reaction of N$_2$O$_5$ with Cl$^-$.

3.2.1. Kinetic Salt Effect. We first consider the effect of added salt when the N$_2$O$_5$ reactant can be modeled as solvated NO$_2^+$ alone rather than as molecular N$_2$O$_5$ or as a neutral NO$_2^+$NO$_3^-$ contact ion pair. In this case, the addition of Na$^+$ and SO$_4^{2-}$ (or Ac$^-$) ions will decrease the rate of ClNO$_2$ formation between the oppositely charged NO$_2^+$ and Cl$^-$ ions by reducing the Coulombic attraction between them. The competing reaction between NO$_2^+$ and H$_2$O is only weakly affected by added ions because one reactant is uncharged.[21]

For singly charged reactant ions such as NO_2^+ and Cl^-, the deceleration in reaction rate has been investigated theoretically by Simonin and co-workers.[22] They show that the diffusion-limited reaction rate between these ions will decrease by only 15% as the ionic strength increases from 0.5 M (for 0.5 M NaCl) to 6.5 M (for 0.5 M NaCl + 2 M Na_2SO_4). This small reduction translates into only a 0.02 reduction in Φ_{ClNO_2}, implying that ionic strength effects lie within our measurement uncertainty.

We can test the prediction of a small ionic strength effect experimentally by measuring Φ_{ClNO_2} as a function of concentration of added $NaClO_4$, which was selected because ClO_4^- is a weakly coordinating anion.[23] Sodium perchlorate was added to 0.5 M $NaCl/D_2O$ solutions in concentrations ranging from 0.0 to 3.0 M (ionic strength of 3.5 M). As shown in Figure 2C, a slight drop in Φ_{ClNO_2} is observed at $NaClO_4$ concentrations below 1.0 M, where it decreases from 0.84 ± 0.03 to a minimum of 0.69 ± 0.08 and then rises to 1.01 ± 0.13 at 3.0 M $NaClO_4$. These small changes contrast sharply with addition of Na_2SO_4 and NaAc. The weak response of Φ_{ClNO_2} to the poorly coordinating ClO_4^- ion and its strong response to added SO_4^{2-} and Ac^- imply that the branching between chlorination and hydrolysis (reactions R2 and R3) is controlled by the specific chemical properties of these added ions and not solely by their concentration (ionic strength). We next explore a potential correlation with one more macroscopic parameter, solution viscosity, before turning to explanations involving specific interfacial and reactive properties of the anions.

3.2.2. Solution Viscosity. The salts Na_2SO_4, NaAc, and $NaClO_4$ each increase the solution viscosity η, but by different amounts. A more viscous medium, in turn, will slow down a diffusion-limited reaction between two solute species such as N_2O_5 and Cl^-, whose rate typically scales as η^{-1}.[21] In parallel, the rate of the solute−solvent hydrolysis of N_2O_5 should also drop with increasing viscosity. Based on studies of isomerization in different viscosity solutions, solute−solvent reactions rates are found to scale as $\eta^{-\alpha}$, with $0 \leq \alpha \leq 1$.[24] When $\alpha = 1$, both reactions R1 and R2 would scale inversely with viscosity, and Φ_{ClNO_2} would not change with η, while Φ_{ClNO_2} would decrease with η if $\alpha < 1$. For the salt concentrations in Figure 2 at 20 °C, η rises from 1.0 to 2.7 centipoise (cP) for 0 to 2 M Na_2SO_4, from 1.0 to 1.17 cP for 0 to 0.5 M NaAc, and from 1.0 to 1.3 cP for 0 to 3 M $NaClO_4$.[25,26] These distinct increments in viscosity do not map onto changes in Φ_{ClNO_2} in Figure 2, as 0.5 M NaAc reduces Φ_{ClNO_2} most strongly but produces the least viscous solution. Subtle variations in the data in Figure 2 may indeed be influenced by changes in η, but the solution viscosity alone does not seem to be a useful parameter for predicting reductions in Φ_{ClNO_2} upon adding salt.

3.2.3. Changes in Near-Surface Chloride Concentration. The trends in Φ_{ClNO_2} in Figure 2 may also arise from changes in Cl^- concentration in the near-interfacial region. We estimate that $ClNO_2$ is formed within the top 30 nm of the air−water interface based on the N_2O_5 reacto-diffusive length

$$l = \sqrt{\frac{D_{aq}}{k_{hyd}}} \tag{E2}$$

assuming an N_2O_5 aqueous diffusion coefficient (D_{aq}) of 1×10^{-5} cm^2 s^{-1} and a lower limit for the N_2O_5 hydrolysis rate constant (k_{hyd}) of 1×10^6 s^{-1}.[27] Recently, Gaston and Thornton[27] estimated that the N_2O_5 reacto-diffusive length is closer to 5 nm for NaCl-containing aerosol, employing a faster N_2O_5 hydrolysis rate. To explain the effects of phenol on Φ_{ClNO_2}, Ryder et al.[10] estimated that the N_2O_5 reacts within the top 1 nm of the interface. As a result, we expect that Φ_{ClNO_2} is extremely sensitive to near-surface availability of Cl^-.

The presence of a strongly surface-active anion could displace Cl^- in the near-surface region, leading to a suppression in Φ_{ClNO_2}. The opposite effect has recently been suggested for cationic surfactants: an increase in N_2O_5 reactivity in the presence of cationic surfactants was attributed to an enhancement in the near-surface concentration of halide ions.[28] In the case of sodium acetate, we observe a slight increase in the surface tension of a 0.5 M $NaCl/D_2O$ solution upon addition of 1.0 M NaAc (Figure 3), suggesting that the
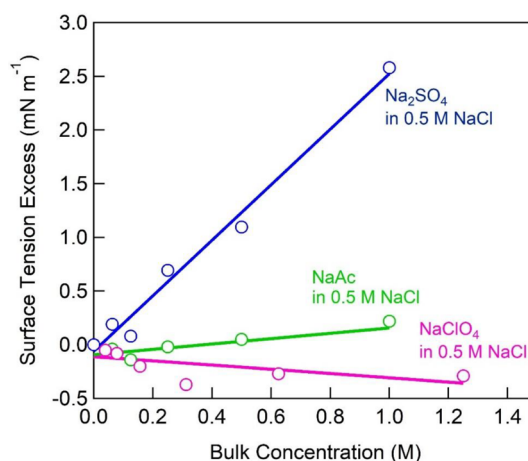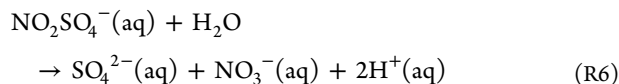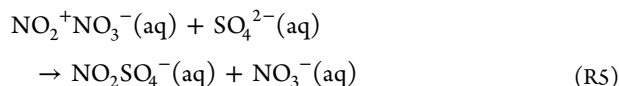

Figure 3. Surface tension of 0.5 M $NaCl/D_2O$ solutions with varying concentrations of sodium sulfate (blue circles), sodium acetate (green circles), and sodium perchlorate (pink circles), each measured at the room temperature of 18 °C.

carboxylate group does not preferentially accumulate near the surface. As expected in the case of a salt containing a doubly charged ion, the surface tension of Na_2SO_4 solutions also increases with increasing sulfate concentration. Hua et al. indicate that chloride is enhanced near the surface relative to sulfate, suggesting that sulfate does not displace chloride from the near surface region where N_2O_5 hydrolysis occurs.[29] The ClO_4^- ion is more surface active than Cl^- or SO_4^{2-},[30] and its minor effect on Φ_{ClNO_2} further supports the view that Cl^- is not substantially excluded from the region in which it reacts.

3.2.4. N_2O_5 Reactions with Added Ions. Perhaps the most likely explanation of the data in Figure 2 involves the possibility that hydrated NO_2^+ (or the $NO_2^+NO_3^-$ ion pair) reacts directly with SO_4^{2-} or Ac^- and H_2O to generate NO_3^- and H^+ and thereby enhances hydrolysis. $ClNO_2$ production is believed to proceed through reaction of NO_2^+ with Cl^- (reaction R2).[3,4] It is thus possible that NO_2^+ (or $NO_2^+NO_3^-$) reacts directly with SO_4^{2-} and Ac^- at a sufficiently fast rate to compete with Cl^- reactions. In the case of sulfate, we hypothesize that the initial reaction forms

the $NO_2SO_4^-$ anion, which quickly hydrolyzes to stable sulfate and nitrate anions:

$$NO_2^+NO_3^-(aq) + SO_4^{2-}(aq)$$
$$\rightarrow NO_2SO_4^-(aq) + NO_3^-(aq) \qquad (R5)$$

$$NO_2SO_4^-(aq) + H_2O$$
$$\rightarrow SO_4^{2-}(aq) + NO_3^-(aq) + 2H^+(aq) \qquad (R6)$$

Ab initio molecular dynamics simulations were carried out to assess the feasibility of these reactions (reactions R5 and R6) relative to the formation of $ClNO_2$ (reaction R2) using methods similar to that employed recently to study reactions of N_2O_4 in small water clusters.[7] Starting with N_2O_5 at the surface of an $(H_2O)_{12}$ cluster solvating one SO_4^{2-} or one Cl^-, we find that reaction proceeds via a $NO_2^+NO_3^-$ transition state. The calculated activation energy barrier for the bimolecular nucleophilic substitution (S_N2) reaction of $NO_2^+NO_3^-$ with SO_4^{2-} is two times smaller ($\Delta H^{\ddagger} = 3.7$ kcal mol^{-1}) than for reaction with Cl^- ($\Delta H^{\ddagger} = 7.4$ kcal mol^{-1}). The lower barrier for reactions R5 and R6 with respect to reaction R2 (Cl^- attack) suggests that $NO_2^+NO_3^-$ reacts even faster with SO_4^{2-} than it does with Cl^-. In this picture, the sulfate ion acts as a catalyst to speed up the normally slower hydrolysis reaction and thereby lowers the $ClNO_2$ branching fraction. A parallel mechanism may also enable acetate to catalyze hydrolysis over chlorination, perhaps through transient formation of acetyl nitrate (CH_3COONO_2) and reaction with water.[31] Lastly, the reaction of $NO_2^+NO_3^-$ with ClO_4^- was computed to be endothermic, indicating that the reaction is not favorable, in accord with its small observed impact on Φ_{ClNO_2}. This lack of reactivity is potentially due to delocalization of the negative charge over all four oxygen atoms in perchlorate. These computational studies lead us to conclude that the steep reductions in Φ_{ClNO_2} with added SO_4^{2-} (and perhaps with Ac^-) arise from the surprising ability of these ions to facilitate hydrolysis over Cl^- attack, a feature that may extend to other ions in aerosol particles as well.

3.3. Relationship between Φ_{ClNO_2} Measured on Thick Films and Submicrometer Aerosol Particles.

To relate measurements of Φ_{ClNO_2} made here using thick aqueous films ($d < 9.5$ mm) to submicrometer aerosol particles ($d < 1$ μm) requires two critical assumptions regarding our experiment: (1) the $ClNO_2$ product from the initial reaction is released to the gas-phase prior to subsequent reaction[3,32,33] and (2) $ClNO_2$ does not undergo further heterogeneous reaction prior to detection via CIMS. In this section we assess the validity of these two approximations.

In our current experiments, we interpret changes in $ClNO_2$ production to be a result of the initial reaction of N_2O_5 with Cl^- and assume that $ClNO_2$ evaporates into the gas phase prior to subsequent reactions. However, if the $ClNO_2$ residence time in the liquid is sufficiently long, hydrolysis and/or secondary reaction with SO_4^{2-} may complicate our interpretation of $ClNO_2$ branching reactions and the link between our experiments conducted on thick films with reactions occurring on suspended aerosol particles. To address these questions, we solve the coupled reaction-diffusion equations for N_2O_5, $ClNO_2$, and NO_2^+ as shown below (eqs E3−E5) to calculate the time-dependent net flux of N_2O_5 and $ClNO_2$ at the surface, J_{net} (N_2O_5) and J_{net} ($ClNO_2$),

respectively (eq E6 and E7). The solubilities (K_H), reaction rates (k), and diffusion constants (D) used in the analysis are included in Table 2.

$$\frac{\partial [N_2O_5]_{(x,t)}}{\partial t} = D\frac{\partial^2 [N_2O_5]_{(x,t)}}{\partial x^2} - k_1[N_2O_5]_{(x,t)} \qquad (E3)$$

$$\frac{\partial [NO_2^+]_{(x,t)}}{\partial t} = D\frac{\partial^2 [NO_2^+]_{(x,t)}}{\partial x^2} + k_1[N_2O_5]_{(x,t)} + k_{-2}[ClNO_2]_{(x,t)}$$
$$- k_2[NO_2^+]_{(x,t)}[Cl^-] - k_3[NO_2^+]_{(x,t)}[H_2O]$$
$$- k_4[NO_2^+]_{(x,t)}[SO_4^{2-}] \qquad (E4)$$

$$\frac{\partial [ClNO_2]_{(x,t)}}{\partial t} = D\frac{\partial^2 [ClNO_2]_{(x,t)}}{\partial x^2} - k_{-2}[ClNO_2]_{(x,t)}$$
$$+ k_2[NO_2^+]_{(x,t)}[Cl^-] \qquad (E5)$$

Table 2. Physical Constants and Reaction Rates Used in the Time-Dependent Model

property or reaction rate	value	reference or footnote
diffusion coefficient (D_{aq}: N_2O_5, $ClNO_2$, NO_2^+)	1×10^{-5} cm^2 s^{-1}	Bertram and Thornton[9]
N_2O_5 solubility (K_H)	2 M atm^{-1}	Bertram and Thornton[9]
$ClNO_2$ solubility (K_H)	0.024 M atm^{-1}	Behnke et al.[3]
N_2O_5 hydrolysis rate (k_1)	1.5×10^5 s^{-1}	Bertram and Thornton[9]
$ClNO_2$ hydrolysis rate (k_{-2})	270 s^{-1}	Behnke et al.[3]
k_2 ($NO_2^+ + Cl^-$)	7.5×10^9 M^{-1} s^{-1}	a
k_3 ($NO_2^+ + H_2O$)	1.6×10^7 M^{-1} s^{-1}	b
k_4 ($NO_2^+ + SO_4^{2-}$)	7.5×10^9 M^{-1} s^{-1}	a

^{a}The reaction rates of $NO_2^+ + Cl^-$ and $NO_2^+ + SO_4^{2-}$ were taken as the diffusion-limited rate constant (k_d) in solution, calculated as $k_d = \frac{8RT}{3\eta}$, where η is the viscosity of water at 298 K.[21] ^{b}The reaction rate of $NO_2^+ + H_2O$ was calculated by scaling k_2 by the experimentally determined ratio of k_2/k_3 determined in Roberts et al.[11]

The following boundary conditions were used for N_2O_5, $ClNO_2$, and NO_2^+.

$$J_{net}(N_2O_5) = J_{in} - J_{des}(t) = \frac{\alpha \langle v \rangle}{4K_HRT}[N_2O_5]^*$$
$$- \frac{\alpha \langle v \rangle}{4K_HRT}[N_2O_5]_{(x=0,t)} \qquad (E6)$$

$$J_{out}(ClNO_2) = -J_{des}(t) = -\frac{\alpha \langle v \rangle}{4K_HRT}[ClNO_2]_{(x=0,t)} \qquad (E7)$$

$$J_{net}(NO_2^+) = 0 \qquad (E8)$$

where $\alpha \langle v \rangle$ is the product of the entry probability and mean velocity, $[N_2O_5]^*$ is the liquid phase concentration of N_2O_5 if fully equilibrated with the gas-phase concentration (here taken as 10 ppb) and we set $[N_2O_5] = [ClNO_2] = [NO_2^+] = 0$ at $t = 0$ for all depths (x). In this analysis, the entry probability (α) was set at 1.

We calculate the $ClNO_2$ branching fraction (Φ_{ClNO_2}) as the ratio of the time-dependent net fluxes of $ClNO_2$ and N_2O_5 at the surface. This approach permits us to assess the effect of solubility, reactivity, and diffusion on $ClNO_2$ branching
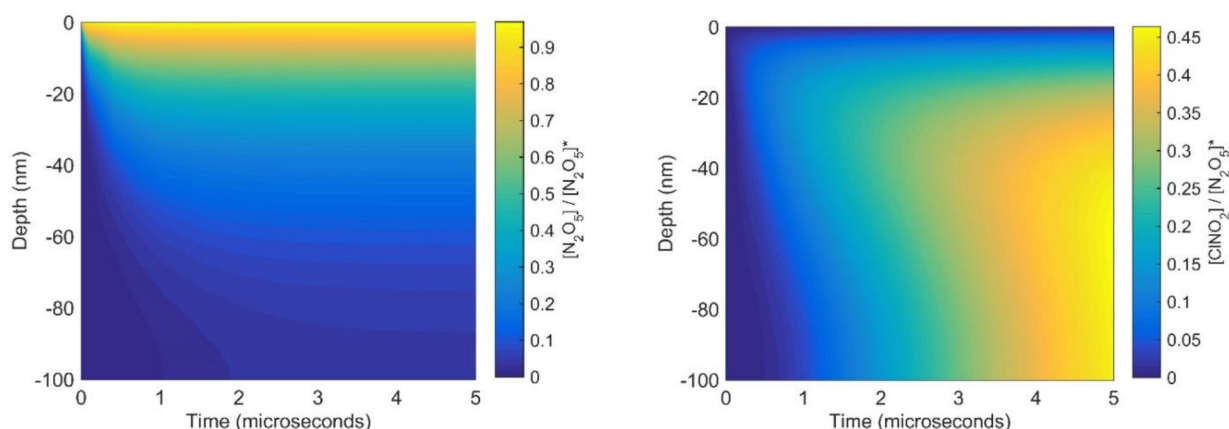
Figure 4. Model calculations of the time and depth dependent concentrations of N_2O_5 (left) and $ClNO_2$ (right) near the air–liquid interface following the reactive uptake of N_2O_5 at the surface ($d = 0$ nm).

fraction and establish a connection between the thick film measurements and suspended aerosol particles. To solve the coupled partial differential equations (PDE) (eqs E3–E5), we utilize the PDE solver in MatLab (pdepe.m) that is based on the finite difference method. We first assess the temporal and spatial patterns of N_2O_5 and $ClNO_2$ in the absence of sulfate (Figure 4). In each figure, the liquid-phase concentrations of N_2O_5 and $ClNO_2$ are normalized to $[N_2O_5]^*$.

As expected, N_2O_5 is primarily confined to the near-surface region ($d < 10$ nm) due to rapid hydrolysis. In contrast, $ClNO_2$ is depleted near the interface due to evaporation to the atmosphere and reaches steady-state within 20 μs at a depth of $d > 60$ nm (Figure 6). To test our model, we can extract the time-dependent solution for $\gamma(N_2O_5)$ from the calculation of $[N_2O_5]_{(x=0,t)}$ and compare it with both the exact analytical solution (eq E9)[34–36] for the case of reversible solubility with irreversible reaction (i.e., N_2O_5 hydrolysis, reaction R1), and the measured values of steady-state $\gamma(N_2O_5)$ for aqueous solutions ($\gamma(N_2O_5) = 0.03$).

$$\frac{\gamma(t)}{\alpha} = \frac{1}{(\tau^{-1} - k)}\left[\sqrt{\frac{k}{\tau}}\, \mathrm{erf}(\sqrt{kt}) + \frac{1}{\tau}\, \mathrm{erfc}\left(\sqrt{\frac{t}{\tau}}\right) e^{(t/\tau - kt)} - k\right]$$

(E9)

where $\tau = D\left(\frac{4K_H RT}{\alpha\langle v\rangle}\right)^2$.

As shown in Figure 5, the analytical solution and the time-dependent model agree well and converge on the steady-state solution of 0.03 after 0.5 μs.

We then calculate the $ClNO_2$ branching fraction, Φ_{ClNO_2}, as the ratio of the net surface fluxes (eq E10).

$$\varphi_{ClNO_2} = \frac{J_{net}(ClNO_2)}{J_{net}(N_2O_5)}$$

$$= \frac{\left(\frac{\alpha\langle v\rangle}{4K_{H,ClNO_2}RT}\right)[ClNO_2]_{(0,t)}}{\left(\frac{\alpha\langle v\rangle}{4K_{H,N_2O_5}RT}\right)\left([N_2O_5]^* - [N_2O_5]_{(0,t)}\right)}$$

(E10)

As shown in Figure 6A, the effective $ClNO_2$ branching fraction achieves a steady-state value of 0.8 by 20 μs, in agreement with Φ_{ClNO_2} calculated from the ratio of the inferred rate constants at 0.5 M NaCl.[3,9,11] For comparison, 20 μs corresponds to a diffusion depth of 100 nm ($\sqrt{D_{aq}t}$). To assess the role of

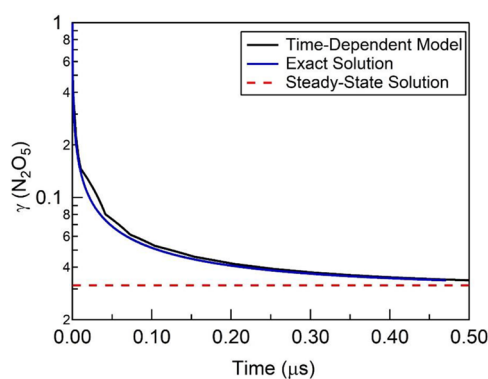**Figure 5.** Time-dependent calculation of $\gamma(N_2O_5)$ using the finite difference model (black), compared with the exact solution for reversible solubility and irreversible reaction (eq E9, blue) and the steady-state solution ($\gamma(N_2O_5) = 0.03$, red dashed line).

sulfate on Φ_{eff} ($ClNO_2$), we set the rate constant for NO_2^+ reaction with SO_4^{2-} (k_4) equal to that with Cl^- (k_2) and to the diffusion-limited rate constant (7.5×10^9 M^{-1} s^{-1}), in accord with the potentially catalytic effect of SO_4^{2-} on both reactions. As expected, Φ_{ClNO_2} is a strongly dependent on $[SO_4^{2-}]$. A comparison of the model with experiment is shown in Figure 7.

To assess the impact of secondary $ClNO_2$ chemistry, which could be amplified due to the thickness of the films used in this study, we set the $ClNO_2$ hydrolysis rate to be 0 s^{-1} and $[SO_4^{2-}] = 1.0$ M. In this case, $ClNO_2$ that is formed in the model is considered inert with respect to secondary chemistry. We then compare the "no $ClNO_2$ hydrolysis" result ($k_{-2} = 0$ s^{-1}) to solutions with varying $ClNO_2$ hydrolysis rates ($0 < k_{-2} < 1.0 \times 10^7$ s^{-1}) in order to assess how fast $ClNO_2$ hydrolysis needs to be for secondary chemistry to impact the measurement of Φ_{ClNO_2} in our system.

Here, we define secondary chemistry to be competitive if the calculated value of Φ_{ClNO_2} is less than 90% of the steady-state solution where $ClNO_2$ hydrolysis is 0 s^{-1} ($\Phi_{ClNO_2} = 0.30$). As shown in Figure 6B, the $ClNO_2$ hydrolysis rate (k_{-2}) would need to be more than 350 times larger than the current recommendation (270 s^{-1}) and more than 15 times larger than the upper bound found in Behnke et al.[3] (6000 s^{-1}) for secondary reactions to be competitive ($\Phi_{ClNO_2} < 0.27$). This calculation indicates that there is no significant effect of $ClNO_2$
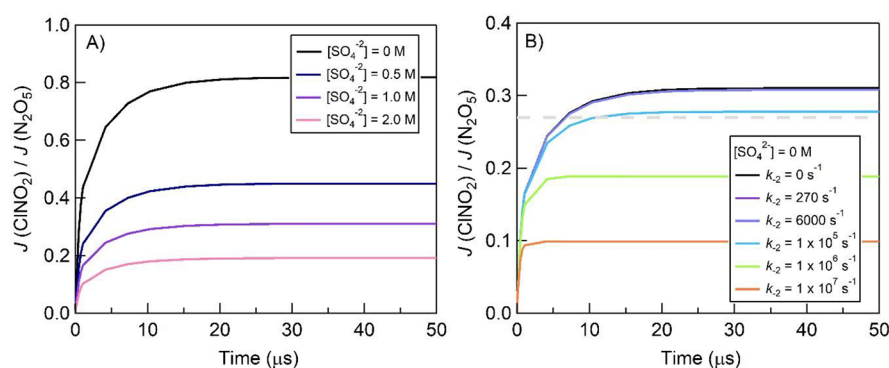
Figure 6. (A)Time-dependent model calculations of Φ_{ClNO_2}, taken as the ratio of the net fluxes of $ClNO_2$ and N_2O_5 at the interface (eq E10). The four curves represent four different bulk concentrations of sulfate. (B) Time-dependent model calculations of Φ_{ClNO_2} for the case of $[SO_4^{2-}] = 1.0$ M, as a function of the prescribed $ClNO_2$ hydrolysis rate (k_{-2}). Solutions for $k_{-2} = 0$, 270, and 6000 s^{-1} are overlapping in (B). The gray dashed line in (B) represents the threshold ($\Phi_{ClNO_2} = 0.27$) below which the hydrolysis of $ClNO_2$ becomes important for determining Φ_{ClNO_2}.
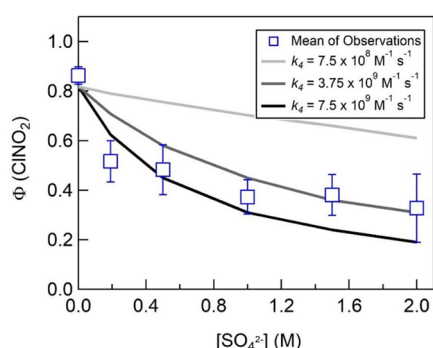

Figure 7. Comparison of average measurements of Φ_{ClNO_2} (blue squares) with the output of the time-dependent model (sampled at 50 μs) using three different rates for the reaction of NO_2^+ with SO_4^{2-}.

hydrolysis and subsequent chemistry in our experiment with a semi-infinite flat slab, unless current estimates of K_H and k_{-2} are in error by orders of magnitude. As a result, we suggest that the effect of SO_4^{2-} (and Ac^-) on Φ_{ClNO_2}, as determined here, is likely present for ambient aerosol containing mixtures of chloride, sulfate, and carboxylates. Nonetheless, the experiments described here should be conducted using an entrained aerosol flow reactor and the kinetics and mechanisms of the aqueous phase reactions should be assessed directly.

Finally, we can compare the output of the time-dependent model to identify a reaction rate for $NO_2^+ + SO_4^{2-}$ (k_4) that is consistent with our observations. As shown in Figure 7, we compare the calculated value of Φ_{ClNO_2} at t = 50 μs for three different values of k_4 (7.5 × 10^8, 3.75 × 10^9, and 7.5 × 10^9 M^{-1} s^{-1}) with the observations described in subsection 3.1. Our results suggest that the reaction rate for NO_2^+ with SO_4^{2-} is approximately equal to that with Cl$^-$ (7.5 × 10^9 M^{-1} s^{-1}) and therefore near the diffusion limit, assuming that the measured reduction in Φ_{ClNO_2} results from this mechanism.

In addition, subsequent heterogeneous reactions of $ClNO_2(g)$ that evaporates from solution, diffuses through the gas phase, and returns to the solution would be interpreted as a reduction in Φ_{ClNO_2}. Following the approach of Knopf et al.,[37] we calculate the loss of $ClNO_2$ from the gas-phase in our flow reactor as a function of the $ClNO_2$ reactive uptake coefficient and the geometry and flow conditions used in this study. In

this approach, only the surface of the aqueous sample is considered reactive (variable γ_{ClNO_2}) and the remaining surface (PTFE or PFA) is unreactive ($\gamma_{ClNO_2} = 0$). For $\gamma_{ClNO_2} = 1.6 \times 10^{-6}$ (0.6 M NaCl),[3] $ClNO_2$ transmission through the flow reactor should be greater than 99%. At $\gamma_{ClNO_2} = 1.0$, $ClNO_2$ transmission is calculated to be 91%, indicating that $ClNO_2$ uptake is diffusion limited. This is consistent with the observed transmission of N_2O_5 through the flow reactor (Figure 1), which was routinely 85−90%. As a result, we do not expect further reactions of $ClNO_2$ to impact our interpretation of Φ_{ClNO_2} in this experiment

3.4. Connecting Laboratory Measurements and Field Observations.
Since the first atmospheric measurements of $ClNO_2$,[5] there has been a significant effort to reconcile atmospheric determinations of Φ_{ClNO_2} with predictions of Φ_{ClNO_2}. In these analyses, predictions of Φ_{ClNO_2} are derived from the laboratory determined dependence of Φ_{ClNO_2} on the ratio of aerosol chloride to water concentrations, using coincident measurements of aerosol chloride mass and calculations of aerosol liquid water content as the input parameters. In both coastal and continental air masses, predictions of Φ_{ClNO_2} generally overpredict atmospheric determinations of Φ_{ClNO_2}.[13,14] Most recently, McDuffie et al.[13] derived over 3000 individual values of Φ_{ClNO_2} in winter nocturnal residual layer over the eastern U.S., by using an iterative box model fit to aircraft observations of O_3, NO_2, N_2O_5, and $ClNO_2$. They showed that predictions of Φ_{ClNO_2} using the k_3/k_2 rate constant ratio from Bertram and Thornton[9] were often more than a factor of 2 larger than the atmospheric determinations derived from the iterative box model. As discussed here and in McDuffie et al., one possibility for the discrepancy is the reaction of NO_2^+ with a competitive anion, e.g. sulfate or acetate, as this reaction competes with $ClNO_2$ formation. McDuffie et al.,[13] using ambient observations, showed that Φ_{ClNO_2} was reduced at high $[SO_4^{2-}]/[H_2O]$ and $[organic]/[H_2O]$ ratios. The dependence of Φ_{ClNO_2} on particulate sulfate and organic material was assessed assuming that $ClNO_2$ formation stems from a two-step reaction mechanism involving dissociation of N_2O_5 to NO_2^+ and subsequent reaction of NO_2^+ with Cl$^-$. Similar to the

experiments of Ryder et al.,[10] it was then assumed that sulfate or organic material could compete for NO_2^+, effectively reducing Φ_{ClNO_2}. In the case of sulfate, the competitive reaction expression for Φ_{ClNO_2}, as derived in the Supporting Information of McDuffie et al.,[13] is determined to be

$$\Phi_{ClNO_2} = \frac{1}{\frac{k_3[H_2O]}{k_2[Cl^-]} + \frac{k_4[SO_4^{2-}]}{k_2[Cl^-]} + 1} \quad (E11)$$

where k_2, k_3, and k_4 refer to reaction of NO_2^+ with Cl^- (eq E2), with water (eq E3), and with any other species such as SO_4^{2-} (eq E4), respectively. eq E11 can be rearranged to the linear eq E12, where the slope of the best fit line in the observations yields the ratio of the reaction rate constants (k_4/k_2) and the intercept, which is equal to the ratio of the reaction rate constants (k_3/k_2):

$$\left(\frac{1}{\Phi_{ClNO_2}} - 1\right)\frac{[Cl^-]}{[H_2O]} = \left(\frac{k_4}{k_2}\right)\left(\frac{[SO_4^{2-}]}{[H_2O]}\right) + \frac{k_3}{k_2} \quad (E12)$$

In McDuffie et al., it was found that the ratio k_4/k_2 needed to be between 1.5 and 19.4 to replicate the field-derived Φ_{ClNO_2} results. However, the intercept (k_3/k_2) was significantly smaller than what laboratory measurements can support. In Figure 8, we reproduce the results of McDuffie et al.[13] and add the laboratory measurements described in this paper to each figure.
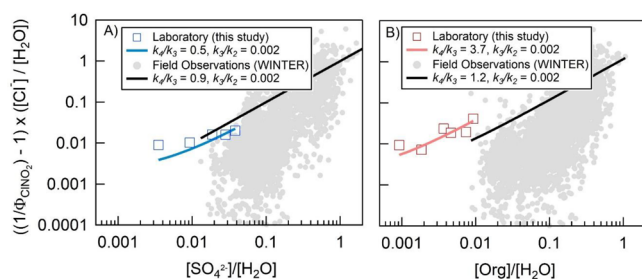

Figure 8. Correlations of $((1/\Phi_{ClNO_2}) - 1)([Cl^-]/[H_2O])$, calculated using an observationally constrained chemical box model with the aerosol sulfate-to-water molar ratio (A) and the aerosol organic-to-water molar ratio (B), as originally shown in McDuffie et al.[13] For the field measurements (gray dots), sulfate aerosol concentrations were calculated from aerosol mass spectrometer (AMS) measurements of aerosol sulfate and thermodynamic calculations of aerosol water. Similarly, organic aerosol concentrations were calculated from measurements of aerosol organic material, assuming a constant organic molecular weight of 250 g mol^{-1}. Laboratory measurements from this study are also shown with blue (A) and red (B) squares for the sulfate and acetate experiments, respectively. The solid lines in each figure are the best fit lines for each data set, constraining the y-intercept ($k_3/k_2 = 0.002$) to the ratio determined in Bertram and Thornton.[9]

As shown in Figure 8, the laboratory measurements presented here are consistent with the interpretation of a competitive reaction pathway for NO_2^+. In the case of NO_2^+ reaction with SO_4^{2-} (k_4) and Cl^- (k_2), the slope (k_4/k_2) derived from the laboratory measurements ($k_4/k_2 = 0.5$) is slightly lower than that shown for the field observations ($k_4/k_2 = 0.9$ when using the aerosol mass spectrometer Cl^- measurements). Perhaps more importantly, the comparison of the ambient determinations with the laboratory measurements highlights how concentrated ambient particles are in

SO_4^{2-}, suggesting that the aqueous phase chemistry involving nitronium ion chemistry discussed here ($[SO_4^{2-}] < 2.0$ M) may not be relevant for all ambient aerosol with high sulfate and/or organic concentrations. In the case of the reaction of NO_2^+ with acetate, the slope of the lines derived from the laboratory and field observations are both positive and of comparable magnitude when the intercept (k_3/k_2) is constrained to that measured in Bertram and Thornton. Future experiments should focus on determining Φ_{ClNO_2} for highly concentrated sulfate and organic aerosol particles.

4. CONCLUSIONS

We report measurements of the dependence of the $ClNO_2$ branching fraction (Φ_{ClNO_2}) on common organic and inorganic aerosol constituents. We find that both sulfate and acetate anions significantly reduce Φ_{ClNO_2} for 0.5 M chloride containing solutions. As shown by comparison to inert sodium perchlorate, these reductions in Φ_{ClNO_2} are not solely a function of solution ionic concentration. Instead, we suggest that sulfate and acetate anions may react directly with N_2O_5 (either as a $NO_2^+NO_3^-$ ion pair or as hydrated NO_2^+) in the near-surface region of the salt solutions. Using a combined reaction and diffusion model, we predict that the rate of reaction between SO_4^{2-} and NO_2^+ in solution would need to be comparable to the reaction between Cl^- and NO_2^+ and therefore near the diffusion-limited rate. The general agreement between laboratory and field determinations of the dependence of Φ_{ClNO_2} on sulfate and acetate suggest that anions other than Cl^- can inhibit the production of $ClNO_2$ in chloride-containing aerosol particles. To definitively determine the role of this chemistry in dictating ambient $ClNO_2$ production, future laboratory studies should focus on direct measurements of Φ_{ClNO_2} to aerosol particles. We expect that incorporation of the dependence of Φ_{ClNO_2} on particulate sulfate and carboxylate into existing parametrizations of $ClNO_2$ heterogeneous chemistry will bring models of $ClNO_2$, and its subsequent chemistry, into closer agreement with recent field observations.

■ ASSOCIATED CONTENT

ⓢ Supporting Information
The Supporting Information is available free of charge on the ACS Publications website at DOI: 10.1021/acsearthspace-chem.9b00177.

Surface tension measurements of salt purity (PDF)

■ AUTHOR INFORMATION

Corresponding Authors
*E-mail: timothy.bertram@wisc.edu.
*E-mail: nathanson@chem.wisc.edu.
ORCID
Joseph R. Gord: 0000-0002-7235-6693
R. Benny Gerber: 0000-0001-8468-0258
Gilbert M. Nathanson: 0000-0002-6921-6841
Timothy H. Bertram: 0000-0002-3026-7588
Present Address
◆E.E.M.: Department of Physics and Atmospheric Science, Dalhousie University, Halifax, NS, Canada.

■ REFERENCES

(1) Ravishankara, A. R. Heterogeneous and Multiphase Chemistry in the Troposphere. *Science* **1997**, *276* (5315), 1058−1065.

(2) Chang, W. L.; Bhave, P. V.; Brown, S. S.; Riemer, N.; Stutz, J.; Dabdub, D. Heterogeneous Atmospheric Chemistry, Ambient Measurements, and Model Calculations of N$_2$O$_5$: A Review. *Aerosol Sci. Technol.* **2011**, *45* (6), 665−695.

(3) Behnke, W.; George, C.; Scheer, V.; Zetzsch, C. Production and Decay of ClNO$_2$ from the Reaction of Gaseous N$_2$O$_5$ with NaCl Solution: Bulk and Aerosol Experiments. *J. Geophys. Res.* **1997**, *102* (D3), 3795.

(4) Finlayson-Pitts, B. J.; Ezell, M. J.; Pitts, J. N. Formation of Chemically Active Chlorine Compounds by Reactions of Atmospheric NaCl Particles with Gaseous N$_2$O$_5$ and ClONO$_2$. *Nature* **1989**, *337* (6204), 241.

(5) Osthoff, H. D.; Roberts, J. M.; Ravishankara, A. R.; Williams, E. J.; Lerner, B. M.; Sommariva, R.; Bates, T. S.; Coffman, D.; Quinn, P. K.; Dibb, J. E.; et al. High Levels of Nitryl Chloride in the Polluted Subtropical Marine Boundary Layer. *Nat. Geosci.* **2008**, *1* (5), 324.

(6) Thornton, J. A.; Kercher, J. P.; Riedel, T. P.; Wagner, N. L.; Cozic, J.; Holloway, J. S.; Dube, W. P.; Wolfe, G. M.; Quinn, P. K.; Middlebrook, A. M.; Alexander, B.; Brown, S. S. A Large Atomic Chlorine Source Inferred from Mid-continental Reactive Nitrogen Chemistry. *Nature* **2010**, *464* (7286), 271−274.

(7) Karimova, N. V.; McCaslin, L. M.; Gerber, R. B. Ion Reactions in Atmospherically-relevant Clusters: Mechanisms, Dynamics and Spectroscopic Signatures. *Faraday Discuss.* **2019**, *217*, 342.

(8) McCaslin, L. M.; Johnson, M. A.; Gerber, R. B. Mechanisms and Competition of Halide Substitution and Hydrolysis in Reactions of N$_2$O$_5$ with Seawater. *Sci. Adv.* **2019**, *5*, eaav6503.

(9) Bertram, T. H.; Thornton, J. A. Toward a General Parameterization of N$_2$O$_5$ Reactivity on Aqueous Particles: The Competing Effects of Particle Liquid Water, Nitrate and Chloride. *Atmos. Chem. Phys.* **2009**, *9* (21), 8351.

(10) Ryder, O. S.; Campbell, N. R.; Shaloski, M.; Al-Mashat, H.; Nathanson, G. M.; Bertram, T. H. Role of Organics in Regulating ClNO$_2$ Production at the Air−Sea Interface. *J. Phys. Chem. A* **2015**, *119* (31), 8519−8526.

(11) Roberts, J. M.; Osthoff, H. D.; Brown, S. S.; Ravishankara, A. R.; Coffman, D.; Quinn, P.; Bates, T. Laboratory Studies of Products of N$_2$O$_5$ Uptake on Cl$^-$ Containing Substrates. *Geophys. Res. Lett.* **2009**, *36* (20), L20808.

(12) Heal, M. R.; Harrison, M. A. J.; Neil Cape, J. Aqueous-Phase Nitration of Phenol by N$_2$O$_5$ and ClNO$_2$. *Atmos. Environ.* **2007**, *41* (17), 3515.

(13) McDuffie, E. E.; Fibiger, D. L.; Dubé, W. P.; Lopez Hilfiker, F.; Lee, B. H.; Jaeglé, L.; Guo, H.; Weber, R. J.; Reeves, J. M.; Weinheimer, A. J.; Schroder, J. C.; Campuzano-Jost, P.; Jimenez, J. L.; Dibb, J. E.; Veres, P.; Ebben, C.; Sparks, T. L.; Wooldridge, P. J.; Cohen, R. C.; Campos, T.; Hall, S. R.; Ullmann, K.; Roberts, J. M.; Thornton, J. A.; Brown, S. S. ClNO$_2$ Yields From Aircraft Measurements During the 2015 WINTER Campaign and Critical Evaluation of the Current Parameterization. *J. Geophys. Res.: Atmos.* **2018**, *123* (22), 12994−13015.

(14) Wang, Z.; Wang, W.; Tham, Y. J.; Li, Q.; Wang, H.; Wen, L.; Wang, X.; Wang, T. Fast Heterogeneous N$_2$O$_5$ Uptake and ClNO$_2$ Production in Power Plant and Industrial Plumes Observed in the Nocturnal Residual Layer over the North China Plain. *Atmos. Chem. Phys.* **2017**, *17* (20), 12361−12378.

(15) Tham, Y. J.; Wang, Z.; Li, Q. Y.; Wang, W. H.; Wang, X. F.; Lu, K. D.; Ma, N.; Yan, C.; Kecorius, S.; Wiedensohler, A.; Zhang, Y. H.; Wang, T. Heterogeneous N$_2$O$_5$ uptake coefficient and production yield of ClNO$_2$ in polluted northern China: roles of aerosol water content and chemical composition. *Atmos. Chem. Phys.* **2018**, *18* (17), 13155−13171.

(16) Kim, M. J.; Farmer, D. K.; Bertram, T. H. A Controlling Role for the Air−sea Interface in the Chemical Processing of Reactive Nitrogen in the Coastal Marine Boundary Layer. *Proc. Natl. Acad. Sci. U. S. A.* **2014**, *111* (11), 3943.

(17) Jimenez, J. L.; Canagaratna, M. R.; Donahue, N. M.; Prevot, A. S. H.; Zhang, Q.; Kroll, J. H.; DeCarlo, P. F.; Allan, J. D.; Coe, H.; Ng, N. L.; Aiken, A. C.; Docherty, K. S.; Ulbrich, I. M.; Grieshop, A. P.; Robinson, A. L.; Duplissy, J.; Smith, J. D.; Wilson, K. R.; Lanz, V. A.; Hueglin, C.; Sun, Y. L.; Tian, J.; Laaksonen, A.; Raatikainen, T.; Rautiainen, J.; Vaattovaara, P.; Ehn, M.; Kulmala, M.; Tomlinson, J. M.; Collins, D. R.; Cubison, M. J.; Dunlea, E. J.; Huffman, J. A.; Onasch, T. B.; Alfarra, M. R.; Williams, P. I.; Bower, K.; Kondo, Y.; Schneider, J.; Drewnick, F.; Borrmann, S.; Weimer, S.; Demerjian, K.; Salcedo, D.; Cottrell, L.; Griffin, R.; Takami, A.; Miyoshi, T.; Hatakeyama, S.; Shimono, A.; Sun, J. Y.; Zhang, Y. M.; Dzepina, K.; Kimmel, J. R.; Sueper, D.; Jayne, J. T.; Herndon, S. C.; Trimborn, A. M.; Williams, L. R.; Wood, E. C.; Middlebrook, A. M.; Kolb, C. E.; Baltensperger, U.; Worsnop, D. R. Evolution of Organic Aerosols in the Atmosphere. *Science* **2009**, *326* (5959), 1525−1529.

(18) Bertram, T. H.; Thornton, J. A.; Riedel, T. P. An Experimental Technique for the Direct Measurement of N$_2$O$_5$ Reactivity on Ambient Particles. *Atmos. Meas. Tech.* **2009**, *2* (1), 231.

(19) Bertram, T. H.; Kimmel, J. R.; Crisp, T. A.; Ryder, O. S.; Yatavelli, R. L. N.; Thornton, J. A.; Cubison, M. J.; Gonin, M.; Worsnop, D. R. A Field-deployable, Chemical Ionization Time-of-Flight Mass Spectrometer. *Atmos. Meas. Tech.* **2011**, *4* (7), 1471−1479.

(20) Kercher, J. P.; Riedel, T. P.; Thornton, J. A. Chlorine Activation by N$_2$O$_5$: Simultaneous, in Situ Detection of ClNO$_2$ and N$_2$O$_5$ by Chemical Ionization Mass Spectrometry. *Atmos. Meas. Tech.* **2009**, *2* (1), 193−204.

(21) Pilling, M. J.; Seakings, P. W. *Reaction Kinetics*; Oxford Science Publications: New York, 1995; Chapter 6.

(22) Simonin, J. P.; Hendrawan, H. Description of Electrolyte Effects on the Kinetics of Reactions Between Ions in Solution, Using the Mean Spherical Approximation. *Phys. Chem. Chem. Phys.* **2001**, *3* (19), 4286−4295.

(23) Strauss, S. H. The Search for Larger and More Weakly Coordinating Anions. *Chem. Rev.* **1993**, *93* (3), 927−942.

(24) Hridya, V. M.; Mukherjee, A. Probing the Viscosity Dependence of Rate: Internal Friction or the Lack of Friction? *J. Phys. Chem. B* **2018**, *122* (39), 9081−9086.

(25) Janz, G. J.; Oliver, B. G.; Lakshminarayanan, G. R.; Mayer, G. E. Electrical Conductance, Diffusion, Viscosity, and Density of Sodium Nitrate, Sodium Perchlorate, and Sodium Thiocyanate in Concentrated Aqueous Solutions. *J. Phys. Chem.* **1970**, *74* (6), 1285−1289.

(26) *CRC Handbook of Chemistry and Physics*, 99th ed.; CRC Press: 2018.

(27) Gaston, C. J.; Thornton, J. A. Reacto-Diffusive Length of N_2O_5 in Aqueous Sulfate- and Chloride-Containing Aerosol Particles. *J. Phys. Chem. A* **2016**, *120* (7), 1039−1045.

(28) Gord, J. R.; Zhao, X. Y.; Liu, E.; Bertram, T. H.; Nathanson, G. M. Control of Interfacial Cl-2 and N2O5 Reactivity by a Zwitterionic Phospholipid in Comparison with Ionic and Uncharged Surfactants. *J. Phys. Chem. A* **2018**, *122* (32), 6593−6604.

(29) Hua, W.; Verreault, D.; Allen, H. C. Relative Order of Sulfuric Acid, Bisulfate, Hydronium, and Cations at the Air-Water Interface. *J. Am. Chem. Soc.* **2015**, *137* (43), 13920−13926.

(30) Hua, W.; Verreault, D.; Allen, H. C. Surface Prevalence of Perchlorate Anions at the Air/Aqueous Interface. *J. Phys. Chem. Lett.* **2013**, *4* (24), 4231−4236.

(31) Louw, R. *Encyclopedia of Reagents for Organic Synthesis: Acetyl Nitrate*; Wiley: 2001.

(32) Frenzel, A.; Scheer, V.; Sikorski, R.; George, C.; Behnke, W.; Zetzsch, C. Heterogeneous Interconversion Reactions of $BrNO_2$, $ClNO_2$, Br_2, and Cl_2. *J. Phys. Chem. A* **1998**, *102* (8), 1329−1337.

(33) Roberts, J. M.; Osthoff, H. D.; Brown, S. S.; Ravishankara, A. R. N_2O_5 Oxidizes Chloride to Cl_2 in Acidic Atmospheric Aerosol. *Science* **2008**, *321* (5892), 1059−1059.

(34) Dempsey, L. P.; Faust, J. A.; Nathanson, G. M. Near-Interfacial Halogen Atom Exchange in Collisions of Cl_2 with 2.7 M NaBr-Glycerol. *J. Phys. Chem. B* **2012**, *116* (40), 12306−12318.

(35) Shi, Q.; Davidovits, P.; Jayne, J. T.; Worsnop, D. R.; Kolb, C. E. Uptake of Gas-phase Ammonia. 1. Uptake by Aqueous Surfaces as a Function of pH. *J. Phys. Chem. A* **1999**, *103* (44), 8812−8823.

(36) Crank, J. *Mathematics of Diffusion*, 2nd ed.; Oxford University Press: London, 1975.

(37) Knopf, D. A.; Poschl, U.; Shiraiwa, M. Radial Diffusion and Penetration of Gas Molecules and Aerosol Particles through Laminar Flow Reactors, Denuders, and Sampling Tubes. *Anal. Chem.* **2015**, *87* (7), 3746−3754.

(38) Towns, J.; Cockerill, T.; Dahan, M.; Foster, I.; Gaither, K.; Grimshaw, A.; Hazlewood, V.; Lathrop, S.; Lifka, D.; Peterson, G. D.; et al. XSEDE: Accelerating Scientific Discovery. *Comput. Sci. Eng.* **2014**, *16* (5), 62−74.